

**Scientific Data Visualization via Hybrid Model based on Fractal Spline Interpolation**

Tayba Arooj  
Department of Mathematics,  
University of the Punjab, Pakistan,  
Email: taybaarroj10@gmail.com

Farsia Hussain  
Punjab University  
College of Information Technology, Lahore, Pakistan,  
Email: farsia.hussain@pucit.edu.pk

Malik Zawwar Hussain  
Department of Mathematics,  
University of the Punjab, Pakistan,  
Email: malikzawwar.math@pu.edu.pk

Received: 01 February, 2019 / Accepted: 12 June, 2019 / Published online: 01 August, 2019

**Abstract.** This research paper is devoted towards the development of a novel hybrid model and its application in the visualization of scientific data. A hybrid model GPRC FIF, based on the spline and fractal interpolation, is established having four parameters and one scaling factor in its description. Data dependent constraints are achieved on two parameters and one scaling factor to envisage the inherit shape (positive) of the data. While two parameters are kept free to provide the shape flexibility to the user. The proposed scheme is also implemented on few numerical data sets to demonstrate the proposed mathematical results graphically. Moreover, the comparative analysis of proposed method with two existing methods is also deliberated.

**AMS (MOS) Subject Classification Codes:** 35S29; 40S70; 25U09

**Key Words:** Hybrid model, Scientific data, Interpolation, Fractal, Spline.

## 1. INTRODUCTION

Data visualization is the major part of scientific studies [5]. The graphical exhibition of data has long been cherished for conveying the message, inferring different data and for having a quick comprehensive view of the data with ease and within no time. Data visualization can be observed in manifold dimensions such as a stock exchange (where the financial drifts can be anticipated), computer graphics, geographic modeling, medical imaging, geology, reverse engineering, oceanography, aerospace firms, hydrology and bio-electrical recording etc.

Data envisioned through classical interpolation manner such as polynomial and spline interpolants, could only provide smooth curves. Particularly, spline interpolation, which has been widely used in data visualization because they are easily constrained and well suited for attaining the smooth structure between the data points. These approaches are effective and functional, widely in designing industrial merchandise only; however, many real phenomena such as coastline, snowflake, surface shapes of mountains etc. have non-smooth (non-linear) configurations and characteristics which cannot be explained by classical interpolation techniques. To address this issue, the method of fractal interpolation is manifested initially by Barnsley [3], grounded on iterated function system (IFS) theory [8]. It is an unconventional technique for analysis data that has non-linear structure. Later, Barnsley & Harrington [4] initiated to introduce differential IFS. Fractal interpolation has been a worthy approach utilized frequently for irregular data visualization but hard to constrain. Therefore, in this study, a novel hybrid model based on fractal and spline interpolation is proposed, that exhibit flexibility in the choice of smooth or non-smooth interpolant in contrast to specific approaches which only yields one structure at a time. The main advantageous feature of the hybrid model over the existing approaches are: (i) they provide a method to render non-smooth approximants (ii) by suitable selection of parameters of the underlying IFS, FIFs can be made smooth and these smooth FIFs include traditional interpolants as special cases (iii) interpolation scheme produced by fractal functions can have local or global dependence on data points, depending on the choice of scaling factors.

A number of authors [2, 5, 9] considered a fractal spline technique to visualize non-linear behavior of data comprehensively. But the core concern in the field of scientific data which the practitioners come across is to visualize rough data in such a manner that the curve should preserve the intrinsic shape. Generally, intrinsic shape of the data is termed as monotone, convex and positive. For instance, blood sugar level, uric acid, hormonal changes, blood pressure and rate of heart beat are a few illustrations of entities having positive values only. Therefore, the required graph should preserve the shape of the data; else it will portray the given sample improperly. Some work on intrinsic shape (positivity) of the data has already been addressed through classical cubic spline for smooth curves [6, 7, 10, 11, 12]. Such problem of visualized the shape of the data in the light of non-linear behavior is studied in this article. In this paper, the problem of positive data visualization is revealed by developing a hybrid model called general piecewise rational cubic (GPRC) fractal interpolation function (FIF) with four free parameters in each sub-interval. General piecewise rational cubic fractal interpolation function (GPRC FIF) generalizes the corresponding traditional GPRC of Hussain and Sarfraz [6] that is highly useful for data visualization. Data dependent conditions are established on two parameters to preserve the

shape of data while two remaining parameters are kept free to transform the shape for the betterment.

## 2. MATERIALS AND METHODS

First, the basic methodology of fractal interpolation function based on iterated function system is discussed. Let the real interval  $I[r_1, r_n]$  has partitioned such that  $r_1 < r_2 < \dots < r_n$ . Further, suppose the data set is given  $(r_i, z_i) \in I \times E : i = 1, 2, \dots, n$ , where  $E$  is denoted as a compact set in  $\mathbb{R}$ . Take  $I_i = [r_i, r_{i+1}]$ , then following two mappings will be contraction homeomorphism such that  $\alpha_i : I \rightarrow I_i$ , with

$$\alpha_i(r_1) = r_i, \alpha_i(r_n) = r_{i+1}, i = 1, 2, \dots, n-1. \quad (2.1)$$

$$|\alpha_i(e_1) - \alpha_i(e_2)| \leq l_i |e_1 - e_2| \forall e_1, e_2 \in I, \text{ for some } 0 < l_i < 1.$$

Assume  $D = I \times E$  and there exist a mapping  $\beta_i : D \times E$ , wish is continuous if

$$\beta_i(r_1, z_1) = z_i, \beta_i(r_n, z_n) = z_{i+1}, i = 1, 2, \dots, n-1.$$

$$|\beta_i(r, y) - \beta_i(r, x)| \leq \kappa_i |y - x|, r \in I, \forall y, x \in E, \text{ for some } -1 < \kappa_i < 1. \quad (2.2)$$

To construct the iterated function system (IFS), a function  $\gamma_i : D \rightarrow D$  is defined as:

$$\gamma_i(r, z) = (\alpha_i(r), \beta_i(r, z)), \forall (r, z) \in D. \quad (2.3)$$

The collection  $\{D; \gamma_i : i = 1, 2, \dots, n-1\}$  is called the iterated function system. The following proposition [3] will assist us in construction of FIF.

**Proposition 2.1.** *The iterated function system (IFS)  $\{D; \gamma_i : i = 1, 2, \dots, n-1\}$  encloses a unique attractor  $G$ , and this attractor is the graph of  $V$ , where  $V : I \rightarrow \mathbb{R}$  is continuous function which interpolates the data  $\{(r_i, z_i) \in I \times E : i = 1, 2, \dots, n\}$ , i.e.,  $V(r_i) = z_i, i = \{1, 2, \dots, n\}$ . The function  $V$  is termed as FIF corresponding to the iterated function system  $\{D; \gamma_i : i = 1, 2, \dots, n-1\}$ , and it may also be generated based on the subsequent.*

Let  $M = \{m | m : I \rightarrow \mathbb{R} \text{ is continuous, } m(r_1) = z_1 \text{ and } m(r_n) = z_n\}$ , where  $M$  is the complete metric space with respect to the uniform metric  $\varphi(m_1, m_2) = \max\{|m_1(r) - m_2(r)| | r \in I\}$ . Define Read-Bajraktarevic operator  $T$  on  $(M, \varphi)$  as:

$$Tm(\alpha_i(r)) = \beta_i(r, m(r)), r \in I, i = 1, 2, \dots, n-1. \quad (2.4)$$

Equation 2.1 and Equation 2.2 ensures that  $Tm$  is continuous on the interval  $[r_i, r_{i+1}]$  and on all the interior points. Also  $T$  is contraction mapping on  $(M, \varphi)$ .

$$\varphi(Tm_1, Tm_2) \leq |\kappa|_\infty \varphi(m_1, m_2),$$

with  $|\kappa|_\infty = \max\{|\kappa_i| : i = 1, 2, 3, \dots, n-1\} < 1$ . Therefore, by Banach fixed point theorem,  $T$  has a unique fixed point  $V$  on  $M$  such that  $T(V(r)) = V(r) \forall r \in I$ . From Equation 2.4, the fractal interpolation function  $V$  fulfills the functional equation

$$V(\alpha_i(r)) = \beta_i(r, V(r)), r \in I, i = 1, 2, \dots, n-1. \quad (2.5)$$

The FIFs generated through the following IFS  $\{D; \gamma_i : i = 1, 2, \dots, n-1\}$

$$\begin{aligned} \alpha_i(r) &= a_i r + b_i, \\ \beta_i(r, z) &= \kappa_i z + F_i(r), \end{aligned} \quad (2.6)$$

with

$$a_i = \frac{r_{i+1} - r_i}{r_n - r_1}, \quad b_i = \frac{r_n r_i - r_1 r_{i+1}}{r_n - r_1}.$$

Where  $\kappa_i$  are called vertical scale factors such that  $|\kappa_i| < 1$ ,  $F_i(r)$  is a continuous function such that  $\beta_i$  satisfies Equation 2.2. The subsequent proposition [4] confirms the presence of a differentiable fractal interpolation function.

**Proposition 2.2.** Suppose the data set  $(r_i, z_i) \in I \times E : i = 1, 2, \dots, n$  with  $r_1 < r_2 < \dots < r_n$ . Further, take  $\alpha_i(r)$  and  $\beta_i(r, z)$  such that satisfying Equation 2.1 and Equation 2.2 respectively. Let for some integer  $g \geq 0$ ,  $|\kappa_i| < a_i^g$ . Assume,  $\beta_i^k(r, z) = \frac{\kappa_i z + F_i^k(r)}{a_i^k}$ , where  $F_i^k$  represents the  $k^{\text{th}}$  derivative with respect to ' $r$ ',

$$z_n^k = \frac{F_1^k(r_1)}{a_1^k - \kappa_1}, \quad z_1^k = \frac{F_{n-1}^k(r_1)}{a_{n-1}^k - \kappa_{n-1}}, \quad k \in 1, 2, 3, \dots, g.$$

If  $\beta_{i-1}^k(r_n, z_n^k) = \beta_i^k(r_1, z_1^k)$ ,  $i = 1, 2, 3, \dots, n-1$ ,  $k \in 1, 2, \dots, g$ , then  $(\alpha_i(r), \beta_i(r, z))$  determines the FIF  $V \in C^g(I)$ , and  $V^k$  is the FIF determined by  $\{(\alpha_i(r), \beta_i^k(r, z)) : i = 1, 2, \dots, n-1\}$ , for all  $k \in 1, 2, 3, \dots, g$ . Since,  $V \in C^1(I)$ ,  $V'$  satisfy the functional equation

$$V'(\alpha_i(r)) = \beta_i^{(1)}(r, V'(r)). \quad (2.7)$$

### 3. A HYBRID MODEL GPRC FIF

Now, the hybrid model (GPRC FIF) with four free parameters is to be developed, made on the IFS Equation 2.6, where the scaling factor  $\kappa_i$  and the polynomial  $F_i(r)$  involved in Equation 2.6 are chosen according to the Proposition 2.2. Suppose the data set  $\{(r_i, z_i) \in I \times E : i = 1, 2, \dots, n\}$  with  $r_1 < r_2 < \dots < r_n$ . Let  $d_i$  be the derivative value at the knot point  $r_i$ . Consider the iterated function system Equation 2.6 with

$$\begin{aligned} F_i(r) &= \frac{p_i(r)}{q_i(r)} = \frac{p_i(\mu)}{q_i(\mu)} \\ &= \frac{A_{1i}(1-\mu)^3 + A_{2i}\mu(1-\mu)^2 + A_{3i}\mu^2(1-\mu) + A_{4i}\mu^3}{\lambda_i(1-\mu)^3 + \delta_i\mu(1-\mu)^2 + \rho_i\mu^2(1-\mu) + \omega_i\mu^3}, \end{aligned} \quad (3.1)$$

where  $\mu = \frac{r-r_1}{r_n-r_1}$ ,  $r \in [r_1, r_n]$ . Here,  $A_{1i}, A_{2i}, A_{3i}, A_{4i}$  are constant and  $\lambda_i, \delta_i, \rho_i, \omega_i$  are the free parameters. To make fixed point  $V$  a  $C^1$  interpolant, the  $C^1$  Hermite conditions are applied. i.e.

$$V(r_i) = z_i, V(r_{i+1}) = z_{i+1}, V'(r_i) = d_i, V'(r_{i+1}) = d_{i+1}.$$

The values of the constants  $A_{1i}, A_{2i}, A_{3i}, A_{4i}$  are evaluated based on above conditions. The conditions  $V(r_i) = z_i$  and  $V(r_{i+1}) = z_{i+1}$  in Equation 2.5 leads to

$$\begin{aligned} A_{1i} &= \lambda_i(z_i - \kappa_i z_1). \\ A_{2i} &= \lambda_i h_i d_i - (r_n - r_1) \lambda_i \kappa_i d_1 + \delta_i(z_i - \kappa_i z_1). \end{aligned}$$

The conditions  $V'(r_i) = d_i$  and  $V'(r_{i+1}) = d_{i+1}$  in Equation 2.7 leads to

$$\begin{aligned} A_{3i} &= -\omega_i h_i d_{i+1} + (r_n - r_1) \omega_i \kappa_i d_n + \rho_i (z_{i+1} - \kappa_i z_n), \\ A_{4i} &= \omega_i (z_{i+1} - \kappa_i z_n). \end{aligned}$$

Substituting the values of  $A_{1i}, A_{2i}, A_{3i}, A_{4i}$  in Equation 3.1, the GPRC FIF is given by

$$V(\alpha_i(r)) = \kappa_i V(r) + \frac{p_i(\mu)}{q_i(\mu)}, \quad (3.2)$$

where

$$\begin{aligned} p_i(\mu) &= \lambda_i (z_i - \kappa_i z_1) (1 - \mu)^3 + (\lambda_i h_i d_i - (r_n - r_1) \lambda_i \kappa_i d_1 \\ &\quad + \delta_i (z_i - \lambda_i z_1)) \mu (1 - \mu)^2 + (-\omega_i h_i d_{i+1} + (r_n - r_1) \omega_i \kappa_i d_n \\ &\quad + \rho_i (z_{i+1} - \kappa_i z_n)) \mu^2 (1 - \mu) + \omega_i (z_{i+1} - \kappa_i z_n) \mu^3, \\ q_i(\mu) &= \lambda_i (1 - \mu)^3 + \delta_i \mu (1 - \mu)^2 + \rho_i \mu^2 (1 - \mu) + \omega_i \mu^3, \\ \mu &= \frac{r - r_1}{r_n - r_1}, z \in [r_1, r_n]. \end{aligned}$$

#### 4. INTERACTIVE PROPERTIES OF GPRC FIF

(i) If  $\kappa_i = 0, \forall i \in \{1, 2, \dots, n-1\}$ , then GPRC FIF shrinks to the classical rational cubic interpolant as:

$$S(r) = \frac{E(\vartheta)}{G(\vartheta)}, \quad (4.1)$$

where

$$\begin{aligned} E(\vartheta) &= \lambda_i z_i (1 - \vartheta)^3 + (\lambda_i h_i d_i + \delta_i z_i) \vartheta (1 - \vartheta)^2 \\ &\quad + (-\omega_i h_i d_{i+1} + \rho_i z_{i+1}) \vartheta^2 (1 - \vartheta) + \omega_i z_{i+1} \vartheta^3, \\ G(\vartheta) &= \lambda_i (1 - \vartheta)^3 + \delta_i \vartheta (1 - \vartheta)^2 + \rho_i \vartheta^2 (1 - \vartheta) + \omega_i \vartheta^3, \\ \vartheta &= (r - r_i) / (r_{i+1} - r_i), \quad r \in [r_1, r_n]. \end{aligned}$$

This shows that if  $\kappa_i \rightarrow 0$ , then the graph of GPRC FIF converts the graph of traditional GPRC given in [4].

(ii) If  $\kappa_i = 0, \lambda_i = \omega_i = 1$  and  $\theta_i = \rho_i = 1$  on each subinterval, then GPRC FIF Equation 3.2 approaches to the standard cubic Hermite spline.

$$\begin{aligned} H(\vartheta) &= (\delta_i \vartheta (1 - \vartheta)^2 + \lambda_i (1 - \vartheta)^3) z_i + (\lambda_i h_i \vartheta (1 - \vartheta)^2) d_i \\ &\quad + (-\omega_i h_i \vartheta^2 (1 - \vartheta)) d_{i+1} + (\rho_i \vartheta^2 (1 - \vartheta) + \omega_i \vartheta^3) z_{i+1}, \end{aligned} \quad (4.2)$$

(iii) GPRC FIF  $\mathbf{V}$  given in Equation 3.2 can be written in the following form

$$\begin{aligned} V(\alpha_i(r)) &= \kappa_i V(r) + [(1 - \mu) z_i + \mu z_{i+1} + \frac{A_i^*(\mu)}{q_i(\mu)}] \\ &\quad - \kappa_i [(1 - \mu) z_1 + \mu z_n + \frac{A_i^{**}(\mu)}{q_i(\mu)}], \end{aligned} \quad (4.3)$$

where,

$$\begin{aligned} A_i^*(\mu) &= h_i\mu(1-\mu)[\mu(\mu\rho_i - \delta_i)\Delta_i\mu(1-\mu) + \lambda_i(1-\mu)(d_i - (1-\mu)\Delta_i) \\ &\quad + \omega_i\mu(\Delta_i\mu - d_{i+1})] \\ A_i^{**}(\mu) &= \mu(1-\mu)[(\rho_i - \delta_i)\Delta_n^*\mu(1-\mu) + \lambda_i h_i(1-\mu)\left(\frac{d_1}{a_i} - (1-\mu)\Delta_n^*\right) \\ &\quad + \omega_i\mu\left(\Delta_n^*\mu - \frac{d_n}{a_i}\right)] \end{aligned}$$

with

$$\Delta_n^* = y_n - y_1.$$

From above equation, it can be easily concluded that the increase of the either one of the parameters  $\lambda_i, \delta_i, \rho_i, \omega_i$ , the  $V$  converges to the following affine FIF

$$V(\alpha_i(r)) = \kappa_i V(r) + (z_i - \kappa_i z_1)(1-\mu) + (z_{i+1} - \kappa_i z_n)\mu.$$

Moreover,  $\kappa_i \rightarrow 0$  then  $V$  approaches to a straight line segment in the interval  $[r_i, r_{i+1}]$ .

## 5. RESULTS AND DISCUSSION

Further, a procedure to develop a positive curve visualization of positive data through a hybrid model (GPRC FIF) described in Equation 3.2 is being presented. Even if the data are positive, random selection of scaling factors and free parameters may not supply precise visualization of the data. Therefore, certain conditions are required on scaling factors and free parameters to acquire a specific shape of the data. The following theorem gives a sufficient condition on free parameters and scaling factor so that FIF preserves inherit (positive) shape of data with the help of [12].

**Theorem 5.1.** *Suppose  $\{(r_i, z_i) : i = 1, 2, \dots, n\}$  be a positive data set such that  $z_i > 0$ . Assuming  $\lambda_i > 0, \omega_i > 0$  and  $d_i$  be the derivative at the knot points  $z_i$ . Then, the hybrid model (GPRC FIF) given in Equation 3.2 preserves inherit (positive) shape of data if the following conditions on scaling factor and free parameters satisfy.*

$$0 \leq \kappa_i < \min\{a_i, \kappa_{1i}^*, \kappa_{2i}^*\}, \delta_i > \max\{0, \delta_i^*\}, \rho_i > \max\{0, \rho_i^*\},$$

where  $\kappa_{1i}^* = \frac{z_i}{z_1}, \kappa_{2i}^* = \frac{z_{i+1}}{z_n}$ ,

$$\delta_i^* = \frac{\lambda_i h_i d_i + (r_n - r_1)\lambda_i \kappa_i d_1}{(z_i - \kappa_i z_1)}, \rho_i^* = \frac{+\omega_i h_i d_{i+1} - (r_n - r_1)\omega_i \kappa_i d_n}{(z_{i+1} - \kappa_i z_n)}.$$

*Proof.* Consider  $V(\rho_i(r)) = \kappa_i V(r) + \frac{p_i(\mu)}{q_i(\mu)}$ , Assuming that  $\kappa_i \geq 0, \forall i = 1, 2, \dots, n$ , then it can be easily observed that  $V(\alpha_i(r)) > 0$  if  $\frac{p_i(\mu)}{q_i(\mu)} > 0$ . As all the free parameters are considered positive, since  $q_i(\mu) > 0$ . So, the positivity of the FIF depends only on numerator  $p_i(\mu)$ . Now from Equation 3.2,  $p_i(\mu)$  can be rewritten as

$$p_i(\mu) = a_{1i}\mu^3 + a_{2i}\mu^2 + a_{3i}\mu + a_{4i}, \quad (5.1)$$

where

$$\begin{aligned} \hat{a}_{1i} &= (\lambda_i + \delta_i)(z_i - \kappa_i z_1) + (\omega_i - \rho_i)(z_{i+1} - \kappa_i z_n) + \lambda_i h_i d_i^* + \omega_i h_i d_{i+1}^*, \\ \hat{a}_{2i} &= (3\lambda_i + 2\delta_i)(z_i - \kappa_i z_1) + (\omega_i - \rho_i)(z_{i+1} - \kappa_i z_n) + 2\lambda_i h_i d_i^* + \omega_i h_i d_{i+1}^*, \\ \hat{a}_{3i} &= (3\lambda_i + \delta_i)(z_i - \kappa_i z_1) + \lambda_i h_i d_i^*, \\ \hat{a}_{4i} &= \lambda_i(z_i - \kappa_i z_1). \end{aligned}$$

With  $d_i^* = (d_i - \frac{\kappa_i}{a_i} d_1)$ ,  $d_{i+1}^* = (d_{i+1} - \frac{\kappa_i}{a_i} d_n)$ . By substituting  $\mu = \frac{\zeta}{\zeta+1}$  in Equation 5.1,  $p_i(\mu) > 0$ ,  $\mu \in [0, 1]$  is equivalent to

$$p_i^*(\zeta) = a_{1i}^* \zeta^3 + a_{2i}^* \zeta^2 + a_{3i}^* \zeta + a_{4i}^*, \quad \forall \zeta > 0. \quad (5.2)$$

Here,

$$\begin{aligned} a_{1i}^* &= \hat{a}_{1i} + \hat{a}_{2i} + \hat{a}_{3i} + \hat{a}_{4i} = \omega_i(z_{i+1} - \kappa_i z_n), \\ a_{2i}^* &= \hat{a}_{2i} + 2\hat{a}_{3i} + 3\hat{a}_{4i} = \omega_i h_i(-d_{i+1} + \kappa_i \frac{d_n}{a_i}) + \rho_i(z_{i+1} - \kappa_i z_n), \\ a_{3i}^* &= \hat{a}_{3i} + 3\hat{a}_{4i} = \lambda_i h_i(d_i - \kappa_i \frac{d_1}{a_i}) + \delta_i(z_i - \kappa_i z_1), \\ a_{4i}^* &= \hat{a}_{4i} = \lambda_i(z_i - \kappa_i z_1). \end{aligned}$$

From [12], we have  $p_i^*(\zeta) > 0$ ,  $\forall \zeta \geq 0$  if and only if  $(a_{1i}^*, a_{2i}^*, a_{3i}^*, a_{4i}^*) \in W_1 \cup W_2$ . Where,

$$\begin{aligned} W_1 &= \{ (a_{1i}^*, a_{2i}^*, a_{3i}^*, a_{4i}^*), \text{ if } a_{1i}^* \geq 0, a_{2i}^* \geq 0, a_{3i}^* \geq 0, a_{4i}^* \geq 0. \}, \\ W_2 &= \begin{cases} (a_{1i}^*, a_{2i}^*, a_{3i}^*, a_{4i}^*), \text{ if } a_{1i}^* \geq 0, a_{4i}^* \geq 0; \\ 4a_{1i}^* a_{3i}^{*3} + 4a_{4i}^* a_{2i}^{*3} + 27a_{1i}^{*2} a_{4i}^{*3} + 27a_{1i}^{*2} a_{4i}^{*2} \\ - 18a_{1i}^* a_{2i}^* a_{3i}^* a_{4i}^* - a_{2i}^{*2} a_{3i}^{*2} \geq 0. \end{cases} \end{aligned}$$

Let  $(a_{1i}^*, a_{2i}^*, a_{3i}^*, a_{4i}^*) \in W_1$ , then we get

$$a_{4i}^* > 0 \Leftrightarrow \kappa_i < \frac{z_i}{z_1}, \quad (5.3)$$

$$a_{3i}^* > 0 \Leftrightarrow \delta_i > \frac{\lambda_i h_i(-d_i + \kappa_i \frac{d_1}{a_i})}{(z_i - \kappa_i z_1)}, \quad (5.4)$$

$$a_{2i}^* > 0 \Leftrightarrow \rho_i > \frac{\omega_i h_i(d_{i+1} - \kappa_i \frac{d_n}{a_i})}{(z_{i+1} - \kappa_i z_n)}, \quad (5.5)$$

$$a_{1i}^* > 0 \Leftrightarrow \kappa_i < \frac{z_{i+1}}{z_n}. \quad (5.6)$$

Due to the rigorous calculation, we omit  $W_2$ . Hence, Equations (5.3-5.6) completes the proof of theorem. This theorem certainly converts hybrid model (GPRC FIF) to positive GPRC FIF.  $\square$

**Corollary 5.2.** If  $\kappa_i = 0$ ,  $\forall i \in \{1, 2, \dots, n-1\}$  in above Theorem 5.1, the sufficient condition convert to  $\lambda_i, \omega_i \geq 0$ ,

$$\delta_i > \frac{\lambda_i h_i d_i}{z_i}, \quad \rho_i > \frac{\omega_i h_i d_{i+1}}{z_{i+1}}.$$

This is sufficient condition of positivity for classical GPRC[6]. The subsequent examples shows the legitimacy that how proposed scheme work for the inherit shape (positive) of the data.

## 6. GRAPHICAL DEMONSTRATION

In the present section we find the numerical simulations of the proposed hybrid model, for distinct values of free parameters and their comparison with two existing models.

This section elaborates the validity and versatility of the proposed model through graphical demonstration of two data sets carry out given below as well as their comparison with two existing models. In these examples, the derivatives values are calculated through arithmetic mean method.

**Example 6.1.** Consider the positive data set enlisted in Table 1. The  $r$ -values represent

TABLE 1. Systolic Blood Pressure

| $i$   | 1   | 2   | 3  | 4   | 5   | 6   | 7   | 8   | 9   | 10  | 11  | 12  |
|-------|-----|-----|----|-----|-----|-----|-----|-----|-----|-----|-----|-----|
| $r_i$ | 5   | 10  | 15 | 20  | 25  | 30  | 35  | 40  | 45  | 50  | 55  | 60  |
| $z_i$ | 186 | 111 | 99 | 102 | 121 | 105 | 110 | 107 | 103 | 104 | 107 | 105 |

time in minutes and  $z$ -values represent systolic blood pressure. The data of Table 1 is demonstrated for random selection of parameters produced the curve in Figure 1 with  $\lambda_i = 0.0091$ ,  $\delta_i = 4.02$ ,  $\rho_i = 0.001$ ,  $\omega_i = 87.01$ ,  $\kappa_i = 0.9$  by Hybrid Model without imposing proposed scheme. It can be easily detected that Figure 1 shows some negative behavior of curve which misguides the observer as the original behavior of the data is throughout positive. To avoid this drawback, Figure 2 (with  $\lambda_i = 0.01$ ,  $\omega_i = 0.3$ ) is generated through the hybrid model with proposed scheme of Theorem 5.1, which preserves the shape of data comprehensively. Figure 3 (with  $\lambda_i = 0.001$ ,  $\omega_i = 0.3$ ) and Figure 4 are also constructed through the aforementioned scheme. Figure 3 not only preserves the shape but also sheds light on its special feature that it can behave like a classical spline by taking all scaling factor equal to zero. Furthermore, Figure 4 reveals the flexibility of the model as one can observe easily that various parameters may lead to different results but preserves the inherit shape.

**Example 6.2.** Consider the positive data set enlisted in Table 2. The  $r$ -values represents

TABLE 2. Creatinine Level in Human Blood

| $i$   | 1    | 2    | 3    | 4   | 5    | 6    |
|-------|------|------|------|-----|------|------|
| $r_i$ | 20   | 30   | 32   | 35  | 37   | 39   |
| $z_i$ | 1.51 | 0.18 | 1.05 | 0.6 | 0.51 | 0.58 |

age and  $z$ -values represent creatinine level in human blood. The continuous data of Table 2 is demonstrated for random selection of parameters produced the curve in Figure 5 with  $\lambda_i = 0.1$ ,  $\delta_i = 22$ ,  $\rho_i = 5$ ,  $\omega_i = 0.1$ ,  $\kappa_i = 0.9$  by Hybrid Model without imposing proposed scheme. It can be easily detected that Figure 5 shows some negative behavior of

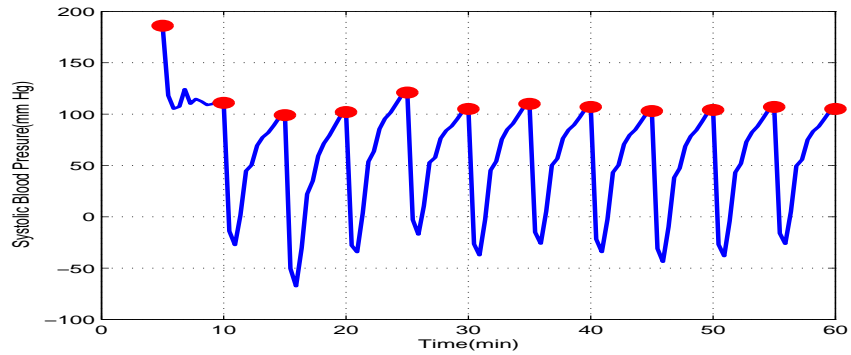


FIGURE 1. Non-Positive Hybrid Model

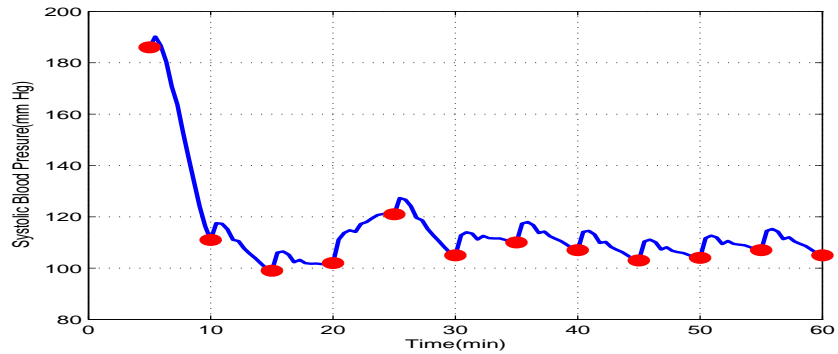


FIGURE 2. Positive Hybrid Model

curve which misguides the observer as the original behavior of the data is throughout positive. To avoid this drawback, Figure 6 (with  $\lambda_i = 0.1, \omega_i = 0.2$ ) is generated through the hybrid model with proposed scheme of Theorem 1, which preserves the shape of data comprehensively. Figure 7 (with  $\lambda_i = 0.0001, \omega_i = 0.0003$ ) and Figure 8 are also constructed through the aforementioned scheme. Figure 7 not only preserves the shape but also sheds light on its special feature that it can behave like a classical spline by taking all scaling factor equal to zero. Furthermore, Figure 8 reveals the flexibility of the model as one can observe easily that various parameters may lead to different results but preserves the inherent shape. So, it is deduced that the execution of proposed scheme is equally efficient for both discrete and continuous data. Hence, one can say that proposed hybrid scheme have more flexibility and applicability.

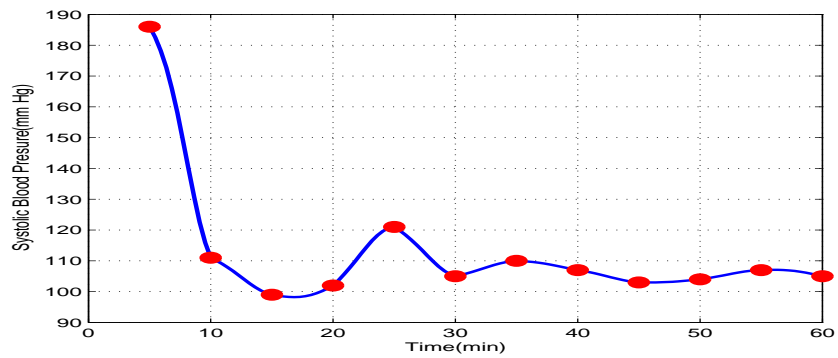


FIGURE 3. Positive Hybrid Model

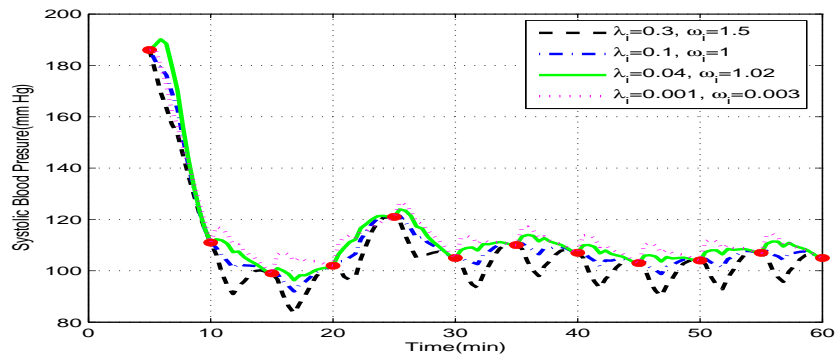


FIGURE 4. Positive Hybrid Model

## 7. COMPARISON ANALYSIS

To ensure the worth of the proposed hybrid model, a comparison of hybrid model after implementation of the proposed scheme with two existing techniques like, a spline [6] and SAFIF [3] is discussed here. For this purpose, two data sets of Table 3 and 4 are chosen

TABLE 3. Positive data

| $i$   | 1  | 2 | 3 | 4   | 5   | 6    | 7    | 8    |
|-------|----|---|---|-----|-----|------|------|------|
| $r_i$ | 1  | 2 | 3 | 8   | 10  | 11   | 12   | 14   |
| $z_i$ | 14 | 8 | 2 | 0.8 | 0.5 | 0.25 | 0.40 | 0.37 |

from [6] to testify the consistency and the validity of the positive GPRC FIF. Figures 7 and 8 are illustrated in the data of Table 3 whereas Figures 9 and 10 are generated through Table 4. Comparing the plots in Figures [7-10], one can identify the drawback of the

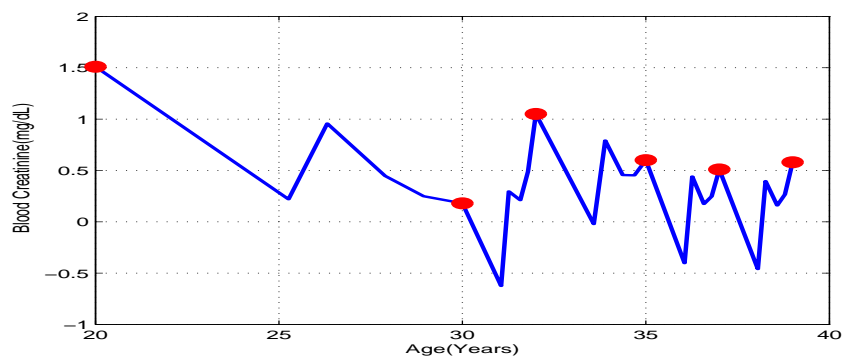


FIGURE 5. Non-Positive Hybrid Model

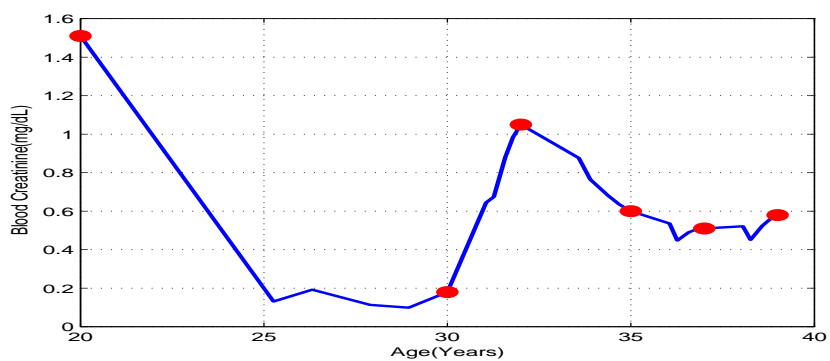


FIGURE 6. Positive Hybrid Model

TABLE 4. HCL and relative conductance

| $i$   | 1  | 2 | 3 | 4 | 5 | 6  | 7  |
|-------|----|---|---|---|---|----|----|
| $r_i$ | 2  | 3 | 7 | 8 | 9 | 13 | 14 |
| $z_i$ | 10 | 2 | 3 | 7 | 2 | 3  | 10 |

existing schemes clearly, as spline model only works smooth positive curves but do not read the non-smooth pattern. SAFIF, On the other hand, read the non-smooth pattern, but does not pledge positive model. However, our proposed positive hybrid model overcome the problem, and work for both positive and non-smooth structure efficiently. Overall, as can be concluded from Figures [7-10], proposed hybrid model give the precise results and could read the inner pattern of data. The results show that the hybrid model is able to yield comparable and better result than the existing two.

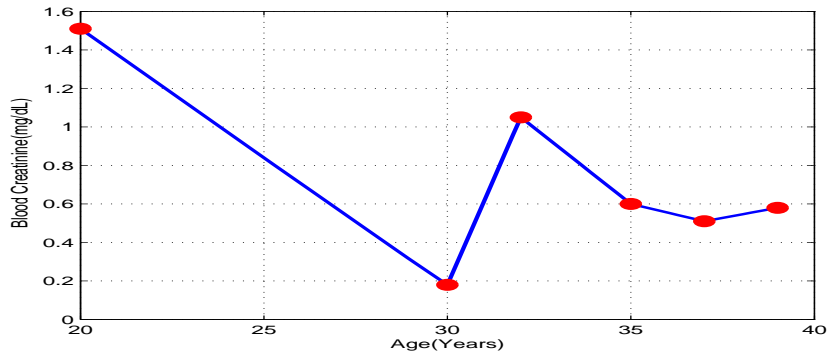


FIGURE 7. Positive Hybrid Model

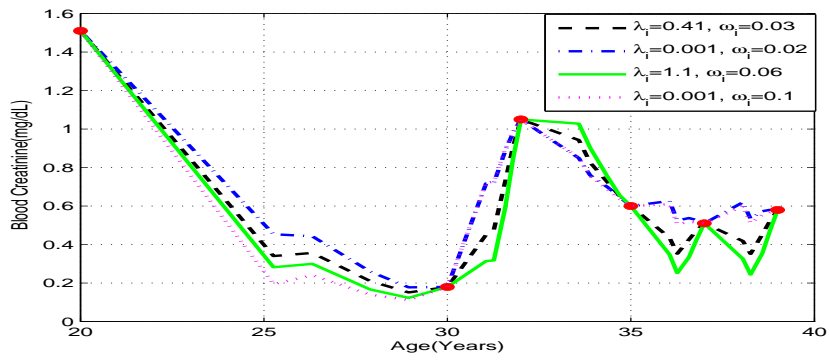


FIGURE 8. Positive Hybrid Model

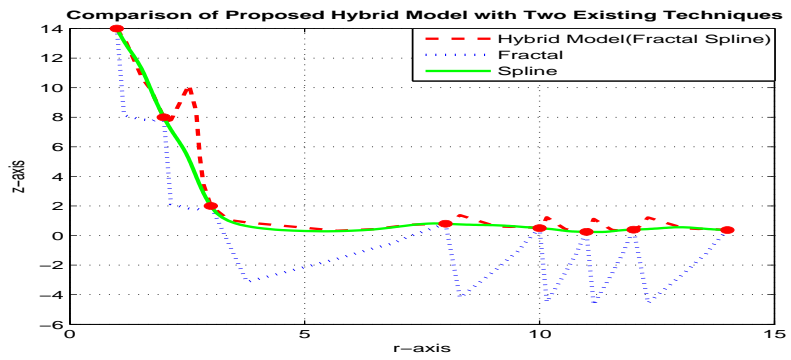


FIGURE 9. 1<sup>st</sup> iteration with choice of parameters  $\lambda_i = \omega_i = 2$ .

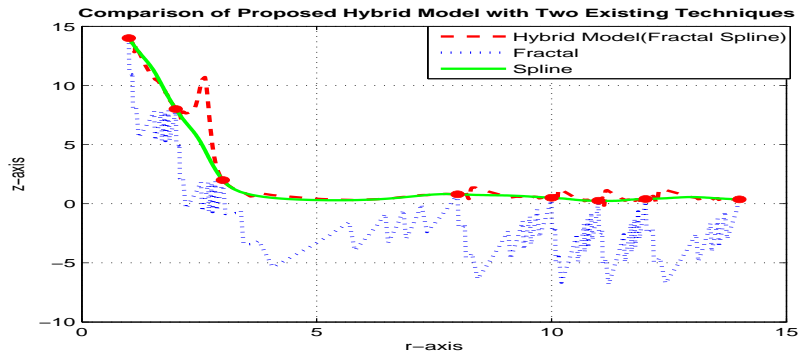


FIGURE 10. 2<sup>nd</sup> iteration with choice of parameters  $\lambda_i = \omega_i = 2$ .

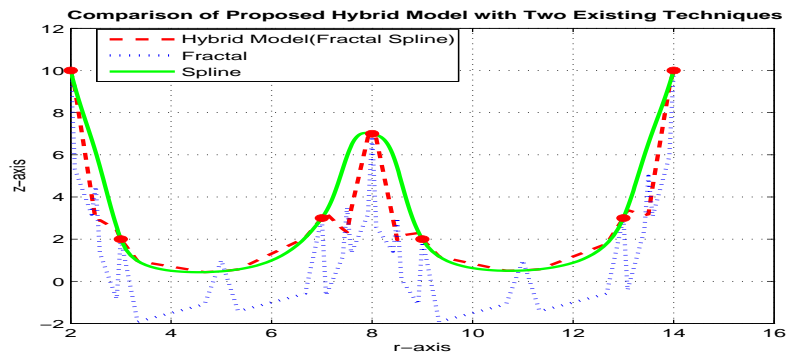


FIGURE 11. 1<sup>st</sup> iteration with choice of parameters  $\lambda_i = \omega_i = 0.5$ .

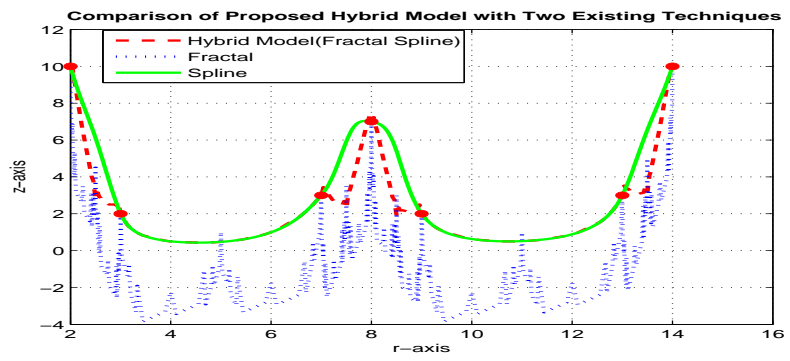


FIGURE 12. 2<sup>nd</sup> iteration with choice of parameters  $\lambda_i = \omega_i = 0.5$ .

## 8. CONCLUSION

The work in this paper is devoted towards the development of the novel hybrid model and its application towards the visualization of scientific data. A hybrid model GPRC FIF, based on the spline and fractal interpolation, is developed along-with four parameters and one scaling factor in its description. Fractal is renowned in non-linear data visualization, whereas spline interpolation is prevalent to achieve particular shape of the data; the combination of these two models enhanced the effectiveness of proposed schemes. Data-dependent constraints are achieved on two parameters and one scaling factor to envisage the inherit shape(positive) of the data. Remaining two parameters are kept free to upsurge tractability. The method described here is considered to be efficient and permits users to enhance required shape of the data. The recommended scheme has numerous exceptional features like it works for both discrete as well as continuous data. It has also a unique degree in each subinterval. In addition, numerical experiments have been conducted to illustrate the feasibility and validity of the proposed method. Finally, the hybrid model is proved to be better than spline and similarly fractal model in nonlinear inherited shape of data visualization.

## 9. ACKNOWLEDGMENTS

The authors are extremely grateful to the referees for providing valuable guidance and comments that helped in improving the manuscript.

## REFERENCES

- [1] S. Abbas, M. Z. Hussain and M. Irshad, *Trigonometric spline for medical image interpolation*, Journal. Natl. Sci. Found. Sri. **45**(1), (2017) 33-40.
- [2] N. Balasubramani, *Shape preserving rational cubic fractal interpolation function*, J Comput. Appl. Math. **319**, (2017) 277-295.
- [3] M. F. Barnsley, *Fractal functions and interpolation*, Constr. Approx. **2**, (1986) 303-329.
- [4] M. F. Barnsley and A. N. Harrington, *The calculus of fractal interpolation functions*, J. Approx. Theory. **57**, (1986) 14-34.
- [5] A. K. B. Chand, N. Vijender and M. A. Navescues, *Shape preserving of scientific data through rational fractal splines*, Calcolo. **51**, (2014) 329-362.
- [6] M. Z. Hussain and M. Sarfraz, *Positivity-preserving interpolation of positive data by rational cubics*, J. Comput. Appl. Math. **218**, (2008) 446-458.
- [7] M. Z. Hussain, F. Hussain and M. Sarfraz, *Shape preserving positive trigonometric spline curves*, Iran. J. Sci. Technol. A. **42**(2), (2016) 763-775. DOI:<https://doi.org/10.1007/s40995-016-0056-1>
- [8] J. E. Hutchinson, *Fractal and self-similarity*, Indiana. U. Math. J. **30**, (1981) 713-747.
- [9] J. Liu and F. Bao, *Visualization of constrained data by smooth rational fractal interpolation*, Int. J. Comput. Math. **93**(9), (2016) 1524-1540.
- [10] M. Sarfraz, M. Z. Hussain and M. A. Ali, *Positivity-preserving scattered data interpolation scheme using the side-vertex method*, Appl. Math. Comput. **218**, (2012) 7898-7910.
- [11] M. Sarfraz, M. Z. Hussain and F. Hussain, *Shape preserving curves using quadratic trigonometric splines*, Appl. Math. Comput. **265**, (2015) 1126-1144.
- [12] J. W. Schmidt and W. Hess, *Positivity of cubic polynomials on intervals and positive spline interpolation*, BIT Numerical Mathematics **28**(2), (1988) 340-352.